Comparative Monte Carlo analysis of InP- and GaN-based Gunn diodes

S. García, S. Pérez, I. Íñiguez-de-la-Torre, J. Mateos, and T. González

Departamento de Física Aplicada, Universidad de Salamanca, Plaza de la Merced s/n, 37008 Salamanca, Spain

In this work, we report on Monte Carlo simulations to study the capability to generate Gunn oscillations of diodes based on InP and GaN with around 1 μm active region length. We compare the power spectral density of current sequences in diodes with and without notch for different lengths and two doping profiles. It is found that InP structures provide 400 GHz current oscillations for the fundamental harmonic in structures without notch and around 140 GHz in notched diodes. On the other hand, GaN diodes can operate up to 300 GHz for the fundamental harmonic, and when the notch is effective, a larger number of harmonics, reaching the Terahertz range, with higher spectral purity than in InP diodes are generated. Therefore, GaN-based diodes offer a high power alternative for sub-millimeter wave Gunn oscillations. © 2014 AIP Publishing LLC.
[http://dx.doi.org/10.1063/1.4863399]

I. INTRODUCTION

In the last decade, the existence of negative differential resistance (NDR)[1–3] in some materials like GaAs or InP has been used by the electronic industry to fabricate vertical structures working as emitters in the millimeter region of the electromagnetic spectrum.[4,5] The generation of waves in the Terahertz (THz) range is not an easy task and several nitride wide-band-gap semiconductors, such as GaN, have attracted the focus of recent researches with the objective of developing sources, amplifiers, and detectors at such high frequencies. GaN-based diodes with a length of the active region of $\sim$ 1 μm have been predicted to provide oscillation frequencies for the fundamental harmonic as high as 200–400 GHz,[6–10] because of its higher saturation velocity with respect to conventional GaAs and InP structures ($v_{sat\_GaN} \approx 1.43 \times 10^7$ cm/s, $v_{sat\_GaAs} \approx 0.9 \times 10^7$ cm/s and $v_{sat\_InP} \approx 1.16 \times 10^7$ cm/s). Potentially, GaN allows increasing the microwave power generation because its threshold electric field is very high: $\sim$200 kV/cm for the Wurzite phase.[11] Although theoretical works predict Gunn oscillations in the THz range in GaN diodes[8,12] experimental demonstrations of oscillations have not been achieved despite technological efforts to fabricate them. It is mostly due to the proximity of the metal contacts and to the high bias required for these devices to work in the NDR conditions which typically causes the diodes to burn out before oscillating.[13,14] Nowadays, as alternative to traditional vertical Gunn diodes, different structures are being explored, highlighting planar structures, such as InGaAs/InAlAs,[15] GaAs/AlGaAs,[16–18] and InGaAs/AlGaAs planar diodes,[19] and GaN/AlGaN self-switching-diodes (SSDs).[20]

In this work, our aim is to present a theoretical comparative study of the amplitude and frequency of the oscillations provided by InP and GaN vertical diodes (with and without notch) by means of a home-made Monte Carlo (MC) simulator[21,22] used to calculate the current power spectral density (PSD) in the diodes.[23] The performance will be studied exploring the effect of the DC bias, the doping profile, and the length of the active region.

The paper is organized as follows. The geometry of the vertical diodes and physical model are described in Sec. II. In Sec. III, the results and discussion are reported: First, we study InP diodes with several lengths for one doping profile. After, we present results obtained in GaN structures for two doping schemes (DS). Some conclusions are finally given in Sec. IV.

II. GEOMETRY OF THE VERTICAL DIODES AND PHYSICAL MODEL

A. Device structure

In this paper, we investigate two types of Gunn diodes, without (n^+nn^+) and with ($n^+n^-nn^+$) notch, sketched in Fig. 1. The diode with notch contains a lightly-doped n^- region adjacent to the cathode, which aims to create a high electric field zone promoting the onset of charge accumulation domains in the cathode. This n^- region has always a fixed length of 250 nm, which is considered to be included in the transit region length L. In both types of structures, the transit or active region is sandwiched between two heavily doped n^+ ohmic contact regions, whose lengths are 100 nm and 300 nm at the cathode and anode, respectively. Systematic MC simulations have been performed accounting for four different lengths of the active region ($L = 1500$ nm, 1200 nm, 900 nm, and 750 nm), two doping levels, and two materials (InP and GaN). The contact regions are always doped at $n^+ = 2 \times 10^{18}$ cm^{-3}. The doping schemes under analysis will be denoted as DS1 and DS2. For the DS1, the transit region is formed by $n = 1 \times 10^{17}$ cm^{-3} and $n^- = 2 \times 10^{16}$ cm^{-3} and for the DS2 by $n = 5 \times 10^{17}$ cm^{-3} and $n^- = 1 \times 10^{17}$ cm^{-3}. Note that for both schemes, the ratio of n/n^- is the same, 5.

B. Semiconductor properties and simulation tool

The intrinsic study of the Gunn structures has been made by means of a semi-classical ensemble MC simulator self-consistently coupled with a 2D Poisson solver.[21] The Poisson equation is discretized by the finite difference method, and
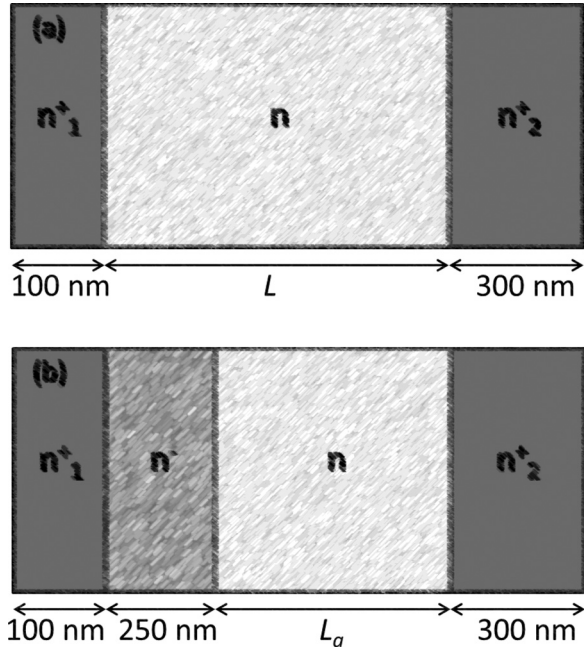
FIG. 1. Geometry of the two types of Gunn structures studied. (a) Diode without notch and (b) diode with a 250 nm-length notch placed next to the cathode. The lengths of n^+ contact regions are 100 nm and 300 nm at the cathode and anode, respectively, in both structures. $n^+ = 2 \times 10^{18}\,cm^{-3}$, DS1: $n = 1 \times 10^{17}\,cm^{-3}$ and $n^- = 2 \times 10^{16}\,cm^{-3}$ and DS2: $n = 5 \times 10^{17}\,cm^{-3}$ and $n^- = 1 \times 10^{17}\,cm^{-3}$. Four different lengths, $L = 1500, 1200, 900$, and 750 nm have been simulated, always at room temperature.

TABLE I. Bulk semiconductor parameters.

Symbol			InP			GaN
Density (kg/m^3)			4790			6150
Sound velocity (m/s)			5130			6560
Static dielectric constant			9.56			5.35
Optic dielectric constant			12.4			8.9
Band gap (eV)			1.344			3.44
Lattice parameter (Å)			5.8687			5.185
Optical phonon energy (meV)			42.2			91.2

	Γ	L	X	Γ_1	U	Γ_3
Effective mass (m*/m$_0$)	0.078	0.26	0.325	0.22	0.39	0.28
No parabolicity coef. (eV^{-1})	0.83	0.23	0.38	0.37	0.5	0.22
Energy from Γ valley (eV)	0.0	0.86	0.96	0	2.2	2.4
Acoustic def. pot. (eV)	6.5	6.5	6.5	8.3	8.3	8.3
Optic def. pot. (eV)	0.0	6.7	0.0	0.0	0.0	0.0
Intervalley def. pot. (10^{10} eV/m)						
From Γ ($\Gamma_{1\,GaN}$) to	0	10	10	0	10	10
From L (U $_{GaN}$) to	10	10	9	10	10	10
From X ($\Gamma_{3\,GaN}$) to	10	9	9	10	10	0
Intervalley phonon energy (meV)						
From Γ ($\Gamma_{1\,GaN}$) to	0	27.8	29.9	0	91.2	91.2
From L (U $_{GaN}$) to	27.8	29.0	29.3	91.2	91.2	91.2
From X ($\Gamma_{3\,GaN}$) to	29.9	29.3	29.9	91.2	91.2	0

the corresponding linear equations are solved by the LU factorization technique. The conduction band of InP and GaN is modeled by three non-parabolic spherical valleys. InP crystallizes under normal conditions in the Zinc-Blende structure, and for this reason Γ, L, and X valleys are considered in our model. Although GaN can crystallize in three types of structures (Wurzite, Zinc-Blende and Rocksalt),[24] we will consider here the Wurzite structure because it is the stable phase of GaN at ambient pressure.[25] In this case, the same model will be used but considering the Γ_1, U, and Γ_3 valleys.[25] The MC simulation parameters for InP and GaN are summarized in Table I.

The scattering mechanisms included in the simulations are intervalley, phonons, acoustic, polar modes (optical and non-optical), and ionized impurities. Furthermore, the piezoelectric scattering mechanism is considered in our GaN model.

Concerning the semiconductor properties GaN can in principle generate higher fundamental oscillation frequencies and power than InP because it has larger saturation velocity, lower energy-relaxation time ($\tau_{GaN} = 0.15$ ps, $\tau_{InP} = 1.7$ ps),[6,26] and higher threshold electric field ($E_{th\_GaN} \approx 200\,kV/cm$, $E_{th\_InP} \approx 13\,kV/cm$).[11,25] As the main objective of this work is to study Gunn oscillations in the frequency domain, the PSD of the current flowing through the device is calculated in order to detect clearly the different harmonics of the signal. To this end, in our case, a specific algorithm to compute the discrete Fourier transform (DFT) based on the fast Fourier transform (FFT) will be used.[23] In this technique, the number of samples (N) of the current history must be an integer power of 2. In our case, the simulations have 150 000 iterations, so we have

considered the last $N = 2^{17} = 131\,072$ samples. The average current value has been subtracted in our dataset to have only into consideration the AC current variation. A time-step Δt of 1 fs is used in the simulations. The frequency resolution, Δf, of the obtained PSD is given by $1/(\Delta tN) = 7.62\,GHz$. The number of electrons simulated is in the range 25 000–50 000 and, if is not indicated, all the results presented in this article are at room temperature.

III. RESULTS AND DISCUSSION

A. InP diodes with DS1

Firstly, the dependence of the current density on the applied bias for InP-based diodes without (w/o) and with notch, for DS1 and different lengths of the active region, $L = 1200$ nm and 1500 nm, are shown in Fig. 2. Gunn instabilities appear once the current saturation is reached, since the main origin of this effect is the onset of intervalley transfer mechanisms.[1–3] In the diodes w/o notch, an abrupt decrease in the average current density for bias of around 5 V is obtained, even if Gunn oscillations are already present for lower voltages. In order to investigate the physical mechanism inside the device that originates the current drop, in the inset of Fig. 2, the time-sequences of current density for $V = 2.5$ V, 5 V, 7 V, and 10 V are plotted for the longer diode. A transition in the oscillation regime at 5 V is observed, from accumulation-layer mode to transit-time dipole-layer mode.[27] In the accumulation-layer mode, the time-sequences of the current density have a sinusoidal-like shape. However, once the transit-time dipole-layer mode appears, the current exhibits an asymmetric nature, thus leading to a decrease in the average current density. In the notched structures, the presence of the higher resistive n^- region lowers the value of the current in the *I-V* characteristics of Fig. 2.
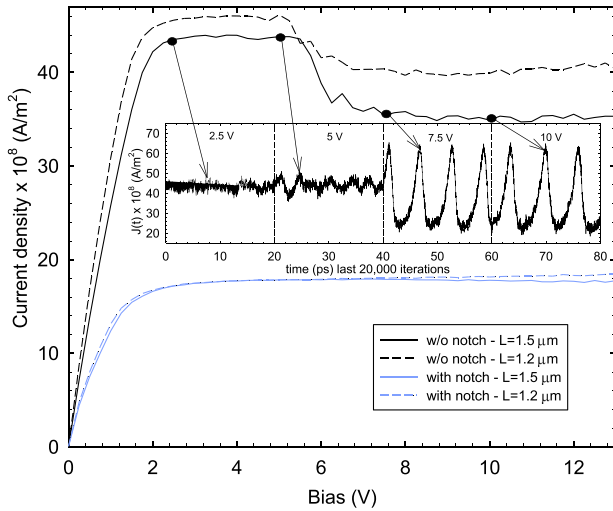
FIG. 2. *I-V* curves for the two types of InP diodes, with and without notch, and for two different lengths of the active region, $L = 1500$ nm and 1200 nm, for the DS1. The inset shows the time-sequences of current density for the structure without notch with $L = 1500$ nm for $V = 2.5$ V, 5 V, 7.5 V, and 10 V.

To study the frequency domain behavior and the spectral purity of the Gunn oscillations obtained, in Fig. 3, the PSD of the current in a diode with $L = 1500$ nm, with and w/o notch is shown when a bias $V = 5$ V is applied. We define the frequency at which the amplitude of the PSD has a remarkable peak as frequency of maximum amplitude, FMA. The notched structure provides higher number of harmonics, $FMA_1 = 152.6$ GHz, $FMA_2 = 297.5$ GHz, $FMA_3 = 450.1$ GHz, and $FMA_4 = 595.1$ GHz for the first, second, third, and fourth harmonic, respectively. The diode w/o notch shows only a clear harmonic with $FMA_1 = 213.6$ GHz. It is noteworthy that the diode with notch offers higher spectral purity but the power of the first harmonic is more than one order of magnitude smaller in comparison with the structure w/o notch, as expected from the lower current level. The frequency and amplitude of the most significant peak of the PSD, FMA_1, versus the bias are represented in Fig. 4. In general, for all devices (not shown here) at low bias FMA_1 lies in the terahertz region and is related to plasmas effects.[28] In particular, for the
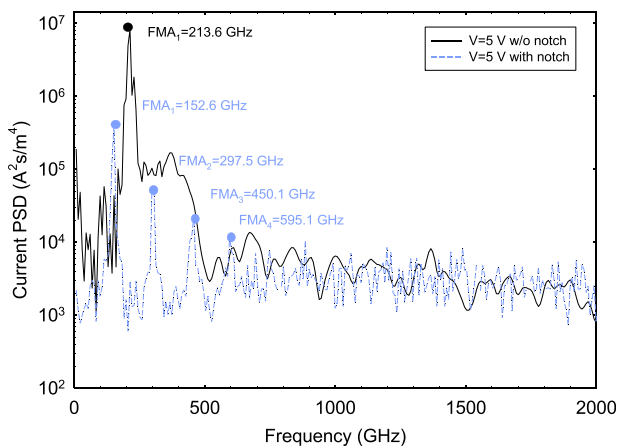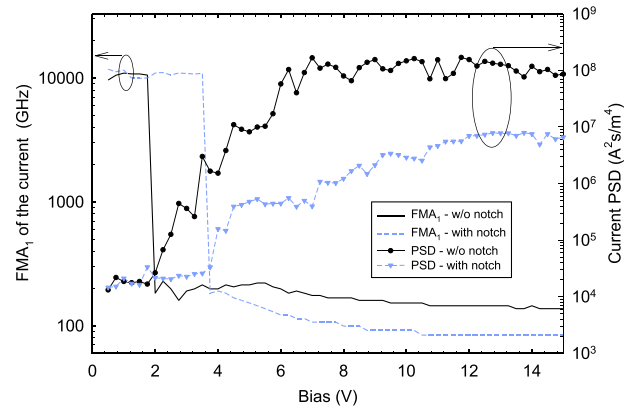

FIG. 4. FMA_1 and corresponding amplitude of the current PSD vs. the bias for InP-based diodes (with and without notch) with $L = 1500$ nm and for the DS1.

structure of Fig. 4, FMA_1 is around 10 THz when the bias is ≤ 3 V. However, as the bias increases, a significant shift of that peak (from high to low frequency) takes place, together with a huge bump in the amplitude. In fact, this strong change of the behavior occurs when Gunn oscillations start, and therefore it is possible to define a threshold voltage, V_{th}, for this effect. For the structure with notch, V_{th} is 3.75 V, and for the diode w/o notch, $V_{th} = 2$ V. In this last device, a saturation of the amplitude of the most significant peak of the current PSD is also observed from a bias around 7.5 V, indicating the existence of a mature oscillation.

The bias dependence of the value of FMA_1 for different lengths of the active region ($L = 1500$ nm, 1200 nm, 900 nm and 750 nm) in diodes with and w/o notch is shown in Fig. 5 for $V > V_{th}$. When the length of the active region is reduced, the frequency obviously increases because carriers travel a smaller distance to reach the anode. In diodes w/o notch, Fig. 5(a), oscillation frequencies are in the range from 130 GHz up to 400 GHz. A more detailed inspection shows that frequency can be estimated as v_{sat}/L_{eff}, being $L_{eff} = L - L_d$, with L_{eff} the effective length and L_d the dead length. We have observed that, irrespectively of the length of the channel, L_{eff} is about 40% of the total length. Thus, the charge accumulation domain is being formed well inside the active region, phenomena already observed in other structures.[29]

Concerning diodes with notch, Fig. 5(b), for lengths of 900 nm and 750 nm, although the condition $n_0 L > 10^{12}$ cm^{-2} is satisfied,[27] Gunn oscillations are not observed. For the longer diodes, lower oscillation frequencies are found, in the range 80–140 GHz. Now, the oscillation frequency can be roughly estimated as v_{sat}/L because the notch creates a high electric field that fixes the domain onset. From the point of view of fabrication, notched devices can easily tune the frequency by designing them with the proper length of the active region. On the other side, for a given length, diodes w/o notch provide higher oscillation frequencies in comparison with structures with notch.

To conclude the study of the InP-based diodes, in Fig. 6, we analyze FMA_n (up to n = 5, if it exists) and its amplitude versus the bias when $L = 1500$ nm. The notched structure provides a higher number of harmonics, but the frequencies
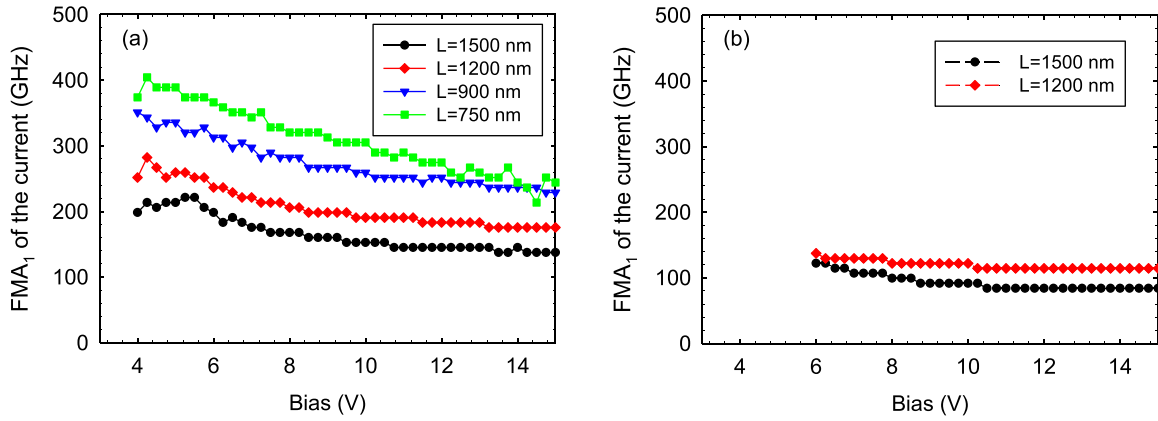

FIG. 3. Current PSD for InP-based diodes (with and without notch) with $L = 1500$ nm for a bias $V = 5$ V.

FIG. 5. FMA_1 for $V > V_{th}$ vs. bias for different lengths of the active region: $L = 1500$ nm, 1200 nm, 900 nm, and 750 nm in an InP-based diode for the DS1. (a) Structures w/o notch and (b) structures with notch.

are lower and also their power (by one or two orders of magnitude). For example, at 10 V in a diode w/o notch, $FMA_3 = 450$ GHz, while in the structure with notch to obtain such high frequency it is necessary to reach the fifth harmonic, $FMA_5 = 442$ GHz. In addition, for the previous case, the structure with notch generates harmonics with higher spectral purity with respect to the diode w/o notch, but the PSD is reduced in a factor ~ 30.

B. GaN diodes with DS1 and DS2

The current PSD for two doping schemes DS1 and DS2 in GaN diodes is presented in Figs. 7(a) and 7(b), respectively, for devices with and w/o notch, $L = 1500$ nm and a bias $V = 80$ V. For DS1, similar current power spectral densities and a strikingly high number of harmonics (reaching ~ 1.8 THz) are achieved in both structures, with and w/o notch. Note that for the InP diode with the same doping scheme (DS1) [Fig. 3] only four harmonics were observed in the notched diode and only the fundamental one in the structure w/o notch. The GaN diode with notch (and DS1) provides a slightly lower FMA_1 (~ 180 GHz) with respect to the structure w/o notch. However, for high order harmonics, the difference between the corresponding FMA_n increases. Note that in contrast with InP, in GaN the amplitude of the

harmonics is very similar for both structures (with and w/o notch). It could indicate that the notch in these devices is not being effective. Hence, in order to boost the effect of the notch in the GaN diodes, a second doping scheme, DS2, where the doping of the n^- and n regions is larger, is considered. The I-V curves for both types of doping (and for $L = 1500$ nm and 1200 nm) are represented in the insets of Figs. 7(a) and 7(b). It is observed that in the case of DS1 [Fig. 7(a)] the notch is not limiting the current, while with the DS2 doping: (i) diodes without notch present a more visible negative incremental resistance zone and (ii) the notch significantly lowers the current in the diodes, as happened in the InP structures with the DS1, so that the saturation current is the same independently of the length. This last effect clearly confirms that DS2 makes the notch more effective. Note that the concentration ratio between the n and n^- regions ($n/n^- = 5$) is the same for DS1 and DS2 but the gradient in the last scheme is higher, thus increasing the electric field in the notch beyond the threshold value ($E_T = 210$ kV/cm). As a consequence, the notch is more effective and it is really fixing the point of formation of the domain close to the cathode. For this reason, like in InP for DS1 where the notch is effective, the PSD and the FMA_1 in notched structures are clearly smaller. For example, FMA_1 are 99 GHz and 140 GHz for structures with and w/o notch, respectively, and, as for InP,
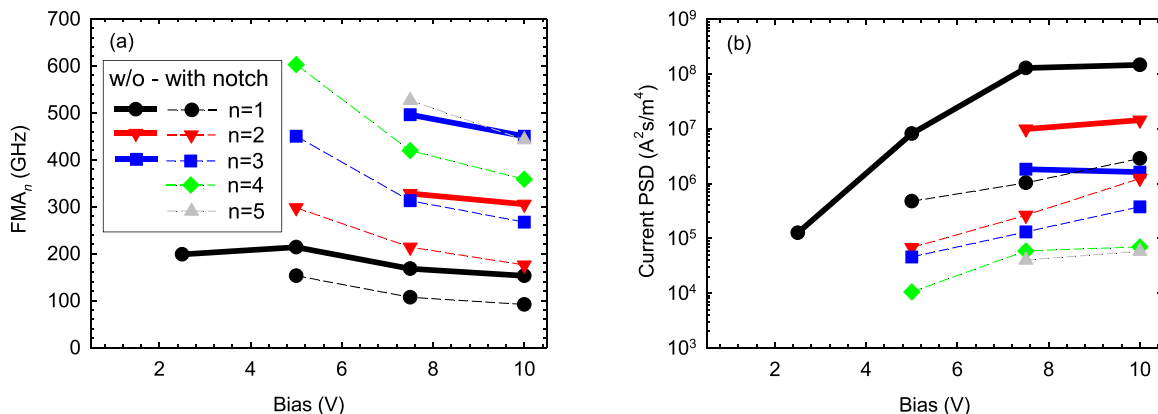

FIG. 6. (a) FMA_n and (b) corresponding amplitude of the PSD for the different harmonics n (up to the fifth if it exists) vs. bias in an InP diode with length $L = 1500$ nm for the DS1. Results in structures with and w/o notch results are represented by dashed and solid lines, respectively.
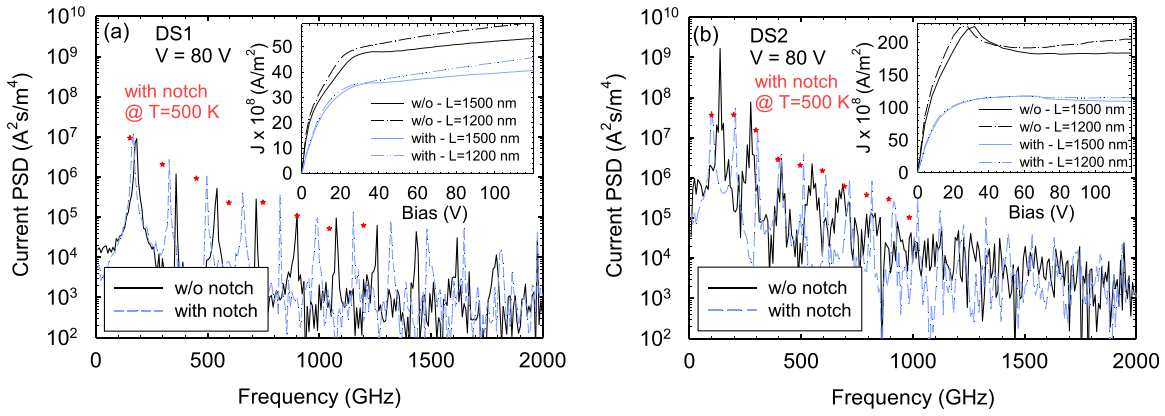
FIG. 7. Current PSD for GaN-based diodes (with and without notch) with $L = 1500$ nm for a bias $V = 80$ V. (a) DS1, (b) DS2. Also, in red star symbols, results for simulations at $T = 500$ K are plotted for the structures with notch. The insets show the I-V curves for both types of diodes and for the two doping schemes analyzed, for $L = 1500$ nm and 1200 nm.

the diode with notch shows a higher number of harmonics (the tenth reaching 1 THz). Furthermore, the current PSD does not decay significantly up to the third harmonic, its extraction being more feasible. Since GaN devices will likely be used for high-power applications, we have studied the high temperature operation of the diode with notch for the two doping schemes. At 500 K, the FMAs are slightly lower for the different harmonics but the PSD does not vary significantly in comparison with the result at room temperature. We now focus the attention only in the third harmonic of the current. The dependence of FMA_3 and the corresponding values of the PSD with the bias are presented in Figures 8(a) and 8(b), respectively, for a diode with length of 1500 nm and DS1 and DS2 doping schemes. Higher values of FMA_3 (460 GHz–580 GHz) are achieved with DS1 in both types of diodes, with and w/o notch, in comparison with DS2, which provides FMA_3 about 280 GHz–442 GHz. The main difference between DS1 and DS2 oscillation frequencies is that while in the first case, the values of FMA_3 in diodes with and w/o notch are very similar, for the DS2 scheme, a larger difference is observed. This fact proves again that the notch for the DS2 is being really effective. The amplitude of the current PSD at FMA_3, Fig. 8(b), is one or two orders of magnitude higher for the DS2, as expected from its higher current

density values. The non-trending data point at 80 V seen in Fig. 8(b) for the DS2 in the structure without notch is attributed to the nonlinearities of the device affecting, in a different way, the noise associated with the dc bias and the oscillating ac component generated by the Gunn effect.

To conclude, Fig. 9 shows the bias dependence of FMA_1 in DS2 diodes for $L = 1500$ nm, 1200 nm, 900 nm, and 750 nm. As described for InP [Fig. 5], when L is reduced, for diodes w/o and with notch, FMA_1 increases, in this case, reaching a maximum value of around 300 GHz. Although GaN diodes were expected to attain higher fundamental frequencies than InP ones, the longer effective transit length L_{eff} observed in GaN structures ($\sim 65\%$) leads to slower Gunn oscillations.

As expected, notched diodes provide lower FMA_1. While for this doping scheme, the condition $n_0 L > 8 \times 10^{12}$ cm^{-2} is fulfilled in all cases,[6,27] note that the structures with notch [Fig. 9(b)] exhibit Gunn oscillations for all lengths and for all bias range, while diodes without notch [Fig. 9(a)] do not oscillate for ≥ 80 V in the case of $L = 750$ nm and 900 nm. Therefore, short notched diodes can generate signals with higher power and very high frequency at upper bias. In this context, it is interesting to study the threshold voltages V_{th} for Gunn oscillations: structures w/o notch exhibit lower values
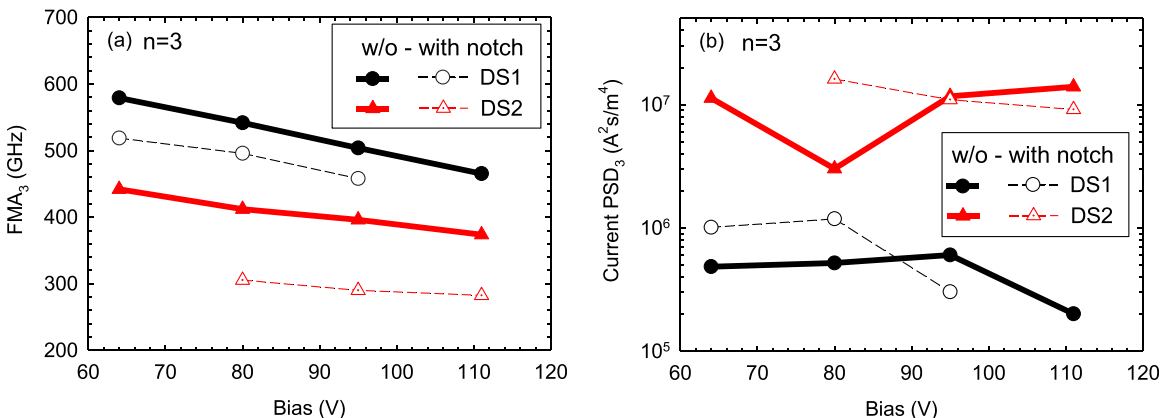

FIG. 8. FMA_3 and (b) corresponding amplitude of the PSD vs. bias in a GaN diode with length $L = 1500$ nm for the DS1 and DS2. Structures with and w/o notch results are represented by dashed and solid lines, respectively.
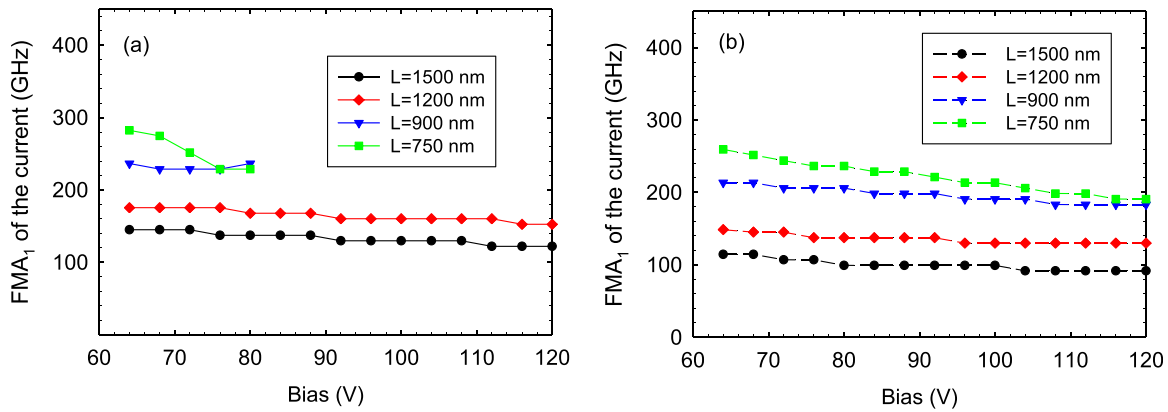
FIG. 9. FMA$_1$ for $V > V_{th}$ vs. the bias for different lengths of the active region ($L = 1500$ nm, 1200 nm, 900 nm, and 750 nm) in a GaN-based diode with DS2. (a) Structures without notch and (b) structures with notch.

of V_{th} and decreasing with L (from 36 V for $L = 1500$ nm to 20 V for $L = 750$ nm), while in the diodes with notch, V_{th} is higher and remains constant with L at 38 V.

IV. CONCLUSIONS

In this work, we have performed a comparative analysis of vertical diodes based on InP and GaN devoted to generate Gunn oscillations. Several active region lengths around one micron and two doping profiles have been considered.

In InP with DS1, the presence of the notch localizes the nucleation of the charge accumulation domain near the cathode and not inside the active region, as happens in the structures without notch. Oscillation frequencies from 130 GHz up to 400 GHz have been achieved in the structures w/o notch. When the bias is increased, lower oscillation frequencies but higher amplitudes of the current PSD are achieved.

In contrast, for the structures of GaN with the same doping scheme, DS1, the notch does not fix the onset of the domain, because the electric field in the notch region is not large enough to promote electrons to the U valley. For this doping scheme, similar frequency and amplitude of the oscillations are achieved in structures with and w/o notch and, interestingly, a large number of harmonics is generated, reaching frequencies up to 1.8 THz. In contrast, for InP-based diodes, only up to the fourth harmonic is observed ($f \sim 600$ GHz) in notched diodes.

With a higher-doping profile (DS2), the notch becomes effective and an even higher number of harmonics with better spectral purity is obtained. And although the FMA$_1$ values are slowly lower (around 300 GHz) than in the devices w/o notch, the amplitude of the power for higher harmonics remains significant up to the THz region. For example, the harmonic number ten with a frequency of 1000 GHz could be feasibly detected. As a general observation, the frequency of Gunn oscillation becomes lower when the DC bias is increased.

ACKNOWLEDGMENTS

[1]J. B. Gunn, Solid State Commun. **1**, 88 (1963).

[2]B. K. Ridley and T. B. Watkins, Proc. Phys. Soc. **78**, 293 (1961).

[3]K. Kurokawa, Bell Syst. Tech. J. **48**, 1937 (1969).

[4]V. Gruzinskis, E. Starikov, P. Shiktorov, L. Reggiani, M. Saraniti, and L. Varani, Simul. Semicond. Devices Processes **5**, 333 (1993).

[5]V. Gruzinskis, E. Starikov, P. Shiktorov, L. Reggiani, and L. Varani, J. Appl. Phys. **76**, 5260 (1994).

[6]E. Alekseev and D. Pavlidis, Solid-State Electron. **44**, 941 (2000).

[7]C. Sevik and C. Bulutay, Appl. Phys. Lett. **85**, 3908 (2004).

[8]R. F. Macpherson, G. M. Dunn, and N. J. Pilgrim, Semicond. Sci. Technol. **23**, 055005 (2008).

[9]V. Gruzinskis, P. Shiktorov, E. Starikov, and J. H. Zho, Semicond. Sci. Technol. **16**, 798 (2001).

[10]R. F. Macpherson and G. M. Dunn, Appl. Phys. Lett. **93**, 062103 (2008).

[11]R. P. Joshi, S. Viswanadha, P. Shad, and R. D. del Rosario, J. Appl. Phys. **93**, 4836 (2003).

[12]C. Sevik and C. Bulutay, Semicond. Sci. Technol. **19**, S188 (2004).

[13]O. Yilmazoglu, K. Mutamba, D. Pavlidis, and T. Karaduman, IEEE Trans. Electron Devices **55**, 1563 (2008).

[14]O. Yilmazoglu, K. Mutamba, D. Pavlidis, and T. Karaduman, Electron. Lett. **43**, 480 (2007).

[15]S. Pérez, T. González, D. Pardo, and J. Mateos, J. Appl. Phys. **103**, 094516 (2008).

[16]A. Khalid, N. J. Pilgrim, G. M. Dunn, C. Holland, C. R. Stanley, I. G. Thayne, and D. R. S. Cumming, IEEE Trans. Electron Devices **28**, 849 (2007).

[17]N. J. Pilgrim, A. Khalid, G. M. Dunn, and D. R. S. Cumming, Semicond. Sci. Technol. **23**, 075013 (2008).

[18]M. Montes, G. Dunn, A. Stephen, A. Khalid, C. Li, D. Cumming, C. H. Oxley, R. H. Hopper, and M. Kuball, IEEE Trans. Electron Devices **59**, 654 (2012).

[19]C. Li, A. Khalid, S. H. Paluchowski Caldwell, M. C. Holland, G. M. Dunn, I. G. Thayne, and D. R. S. Cumming, Solid-State Electron. **64**, 67 (2011).

[20]A. Íñiguez-de-la-Torre, I. Íñiguez-de-la-Torre, J. Mateos, T. González, P. Sangaré, M. Gaucher, B. Grimbert, V. Brandli, G. Ducournau, and C. Gaquière, J. Appl. Phys. **111**, 113705 (2012).

[21]C. Jacoboni and P. Lugli, *The Monte Carlo Method for Semiconductor Device Simulation* (Springer-Verlag, New York, 1989).

[22]A. Íñiguez-de-la-Torre, J. Mateos, and T. González, J. Appl. Phys. **107**, 053707 (2010).

[23]W. H. Press, B. P. Flannery, S. A. Teukolsky, and W. T. Vetterling, *Numerical Recipes. The Art of Scientific Computing* (Cambridge University Press, New York, 1989).

[24]E. López and J. Arriaga, Superficies Vacío **17**(1), 21 (2004), available at http://www.redalyc.org/articulo.oa?id=94217105.

[25]O. Madelung, *Semiconductors: Data Handbook*, 3rd ed. (Springer-Verlag, New York, 2004).

[26]G. H. Glover, Appl. Phys. Lett. **21**(9), 409 (1972).

[27]S. M. Sze and K. K. Ng, *Physics of Semiconductor Devices*, 3rd ed. (Wiley & Sons, Inc., Publication, New Jersey, 2007).

[28]L. Reggiani, P. Golinelli, E. Faucher, L. Varani, T. González, and D. Pardo, in Proceedings of the 13th International Conference of Noise in Physical Systems and 1/f Fluctuations, edited by V. Bareikis and R. Katilius, (World Scientific, Singapore, 1995), Vol. 193.

[29]Y. Wang, L. Yang, W. Mao, S. Long, and Y. Hao, IEEE Trans. Electron Devices **60**, 1600 (2013).